Supplementary Information

Performant flexible luminescent solar concentrators of phenylpolysiloxanes crosslinked with perylene bisimide fluorophores

Elisa Della Latta,[1] Francesca Sabatini,[1] Cosimo Micheletti,[1] Marco Carlotti,[1] Francesca Martini,[1] Francesca Nardelli,[1] Antonella Battisti,[2] Ilaria Degano,[1,3] Marco Geppi,[1,3] Andrea Pucci[1,3,], Svenja Pohl[4], Guido Kickelbick[4]*

[1]*Deparment of Chemistry and Industrial Chemistry, University of Pisa, Via Giuseppe Moruzzi 13, 56124 Pisa, Italy*
[2]*Nanoscience Institute, CNR and NEST, Scuola Normale Superiore, P.zza S. Silvestro 12, 56127 Pisa, Italy*
[3]*CISUP, Centro per l'Integrazione della Strumentazione dell'Università di Pisa, Lungarno Pacinotti 43, I-56126 Pisa, Italy*
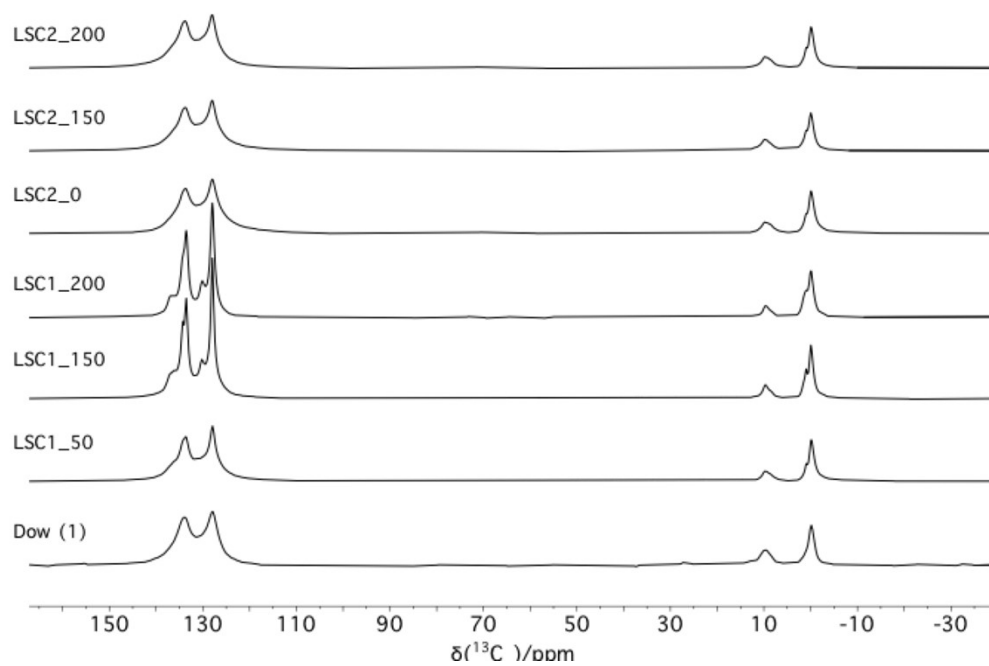[4]*Saarland University, Inorganic Solid-State Chemistry, Campus, Building C4 1, 66123 Saarbrücken, Germany*
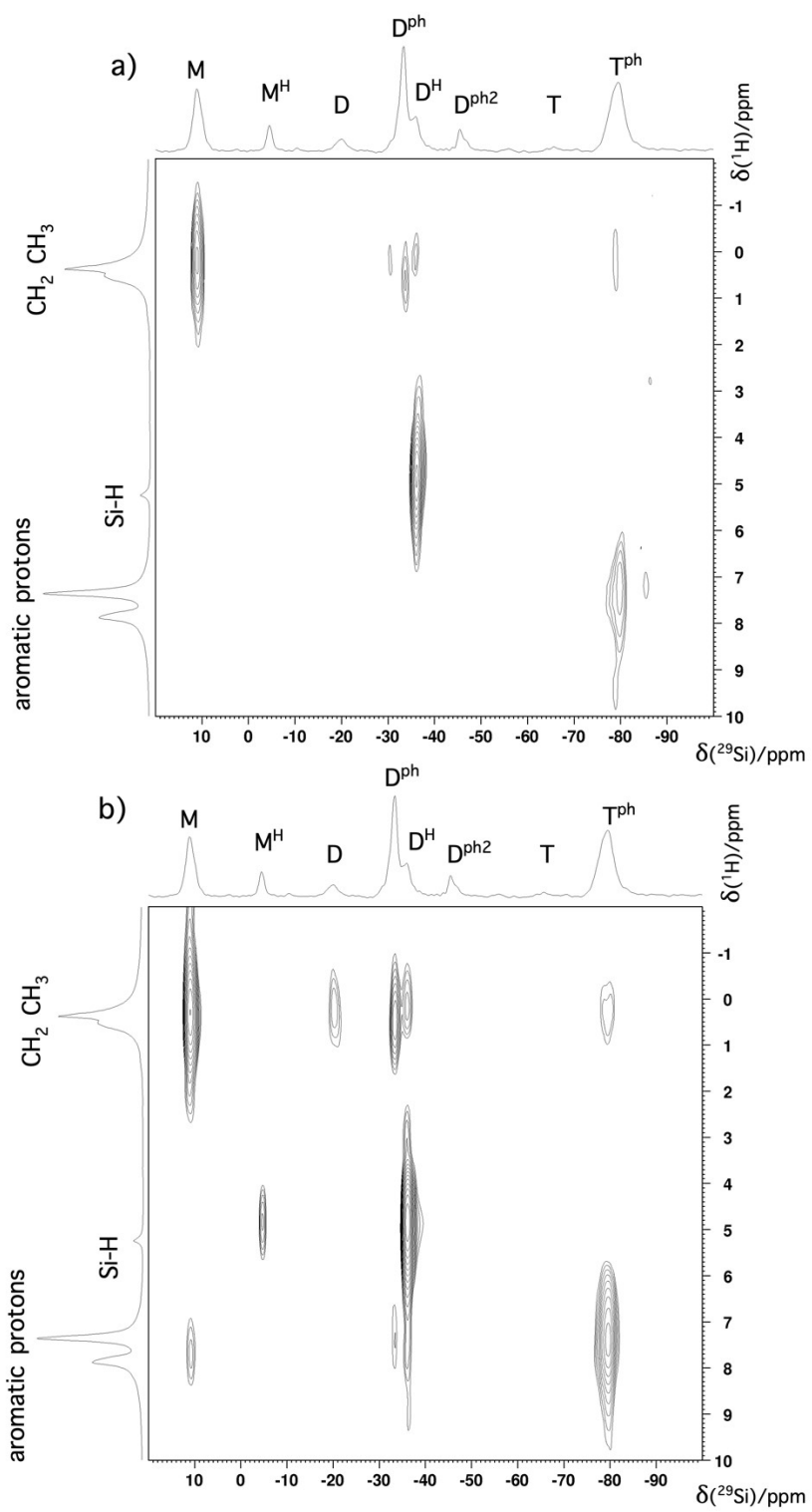
corresponding author(s)
Dr. Francesca Martini, email: francesca.martini@unipi.it
Prof. Andrea Pucci, email: andrea.pucci@unipi.it

Solid-State NMR

Figure S1: ^{13}C DE/MAS spectra of LSC1 and LSC2 samples.

**Figure S2**. 2D ^{1}H-^{29}Si HETCOR spectra of LSC1_50 recorded with ct of 500 µs (a) and 1500 µs (b).

¹H – ²⁹Si 2D HETCOR spectra

2D ¹H-²⁹Si HETCOR experiments were performed on LSC1_50 to further validate the assignment of ¹H and ²⁹Si 1D spectra and obtain additional structural information. In Figure S2 two HETCOR spectra recorded with two different contact times (ct = 0.5 and 1.5 ms) are reported, capable to monitor spatial closeness between ²⁹Si and ¹H nuclei over two slightly different spatial scales. The main peaks confirm the assignments previously reported for ¹H and ²⁹Si peaks and the main features of the structure of LSC. Interestingly, a correlation between the signals of T^{ph} silicon atoms (-80 ppm) and methyl and methylene protons (0.5 ppm) is observed. This indicates that T^{ph} atoms are close in the structure to silicon atoms bonded to methyl and methylene groups. Moreover, the 2D spectrum recorded with the longest ct also shows a correlation between M groups (11 ppm) and aromatic protons (7.5 ppm), indicating that M silicon atoms are quite close in the structure to D^{ph} and T^{ph} groups.

PY-GC/MS

Analyses were performed using an EGA/PY-3030D micro-furnace pyrolizer coupled to an 8890 gas and a 5977 Mass Selective Detector (Agilent Technologies, USA). Irradiation of the samples was performed with an UV-1047 Xe micro UV-irradiator and a QSP-1046E quick-stabilizing pressure flow switch (Frontier Laboratories Ltd., Japan). This instrument has been described in previous publications. The micro-UV irradiator is equipped with a Xe arc lamp, with emission in the range of 280–450 nm. The irradiance of emitted light was approximately 3000 W/m². Irradiation took place directly inside the pyrolysis furnace at a temperature of 60 °C. To simulate natural irradiation conditions, the carrier gas was switched to air during UV exposure. After irradiation, carrier gas was switched back to helium and the system was purged for 15 min before analysis. The irradiation time was 1 h. After irradiation and purging, the

samples were pyrolyzed at 600 °C for 0.2 min. The pyrolizer interface and GC injector were operated at 280 °C and injection was performed with a 10:1 split ratio. Separation of the pyrolysis products was achieved with an HP-5MS fused silica capillary column (95% dimethyl, 5% phenyl polysiloxane, 30 m x 0.25 mm, film thickness 0.25 μm, Agilent Technologies, USA) and helium as carrier gas (1 mL min^{-1}). The chromatographic program was: initial temperature 40 °C for 5 min, 10 °C/min to 310 °C for 20 min. The mass spectrometric detector was operated in EI positive mode (70 eV) scanning in the range from 35 to 600 m/z. The ion source was kept at 230 °C, while the quadrupole analyzer was kept at 150 °C. The data collected were interpreted by the NIST Mass Spectral Search Program (version 2.0).
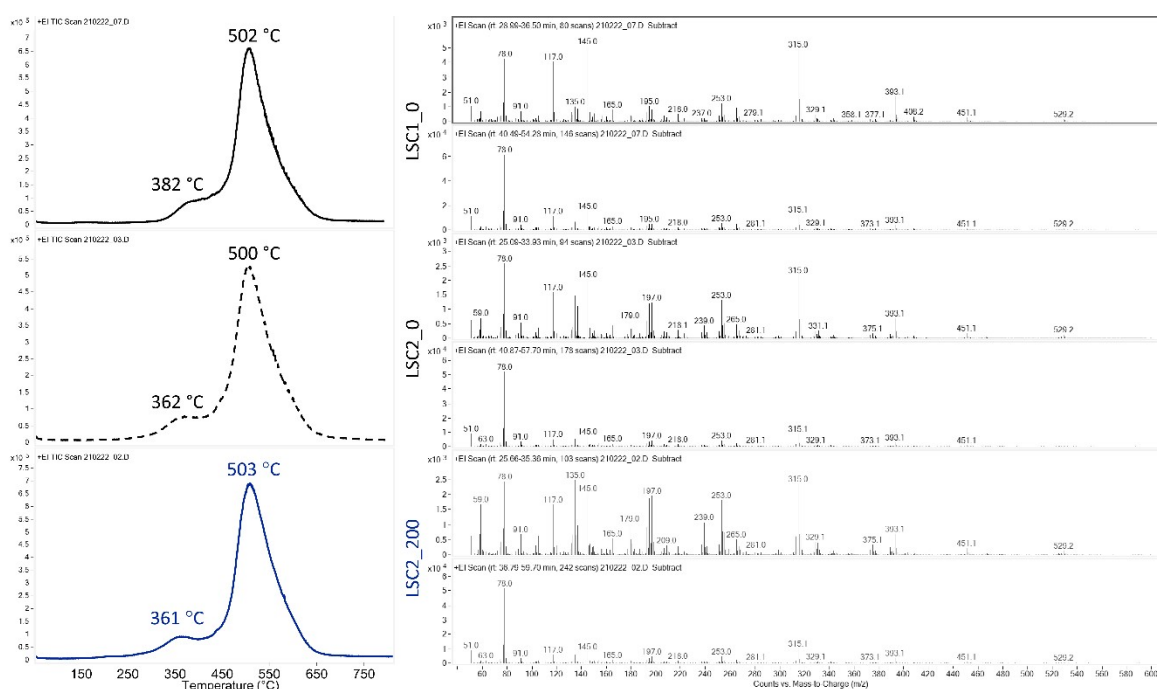
Figure S3. Total Ion Thermograms (TIT) with mass spectra corresponding to the two evolution bands, obtained for samples LSC1_0, LSC2_0, and LSC2_200.
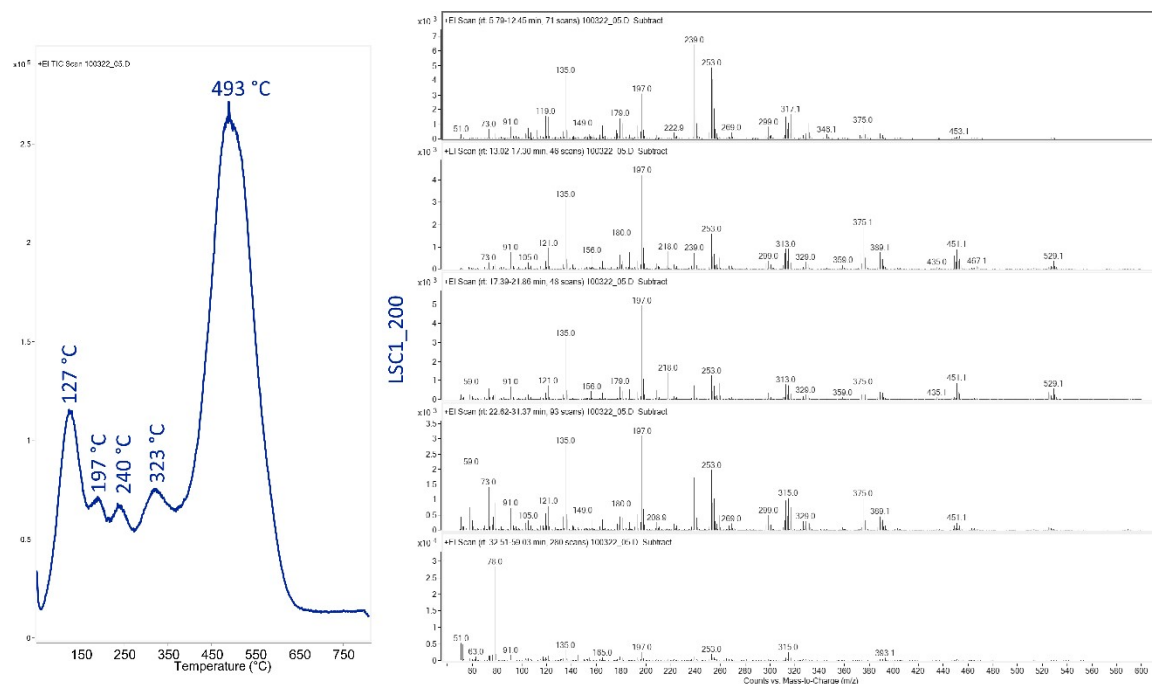
Figure S4. Total Ion Thermograms (TIT) with mass spectra corresponding to the four evolution bands, obtained for sample LSC1_200.

Table S1. Peaks identified in the chromatograms shown in Figure 7. Peaks labelled with Roman numerals are only present in the dye-containing sample LSC1_200.

#	tr (min)	Compound	LSC1_0	LSC1_200	LSC2_0	LSC2_200
1	3.7	Benzene	x	x	x	x
2	5.1	Toluene	x	x	x	x
3	5.9	1-Octene	x	-	-	-
4	6.7	2,2,5,5-Tetramethyl-2,5-disilaoxolane	x	x	x	x
5	7.0	Hexamethylcyclotrisiloxane	x	x	x	x
6	7.7	Hex-1-enylbenzene	x	-	x	x
7	7.9	Ethylbenzene	x	-		
8	8.4	Styrene	x	x	x	x
9	9.4	Silane, dimethylphenyl-	x	x	x	x
10	9.5	Benzaldehyde	x	x	-	-
11	9.7	Benzonitrile	x	x	-	-
12	9.8	Phenol	x	x	-	-
13	10.0	Octamethylcyclotetrasiloxane	x	x	-	-
14	10.1	Silane, trimethylphenyl-	x	x	-	-
I	10.3	1-Hexanol, 2-ethyl-	-	x	-	-
15	10.5	Benzene, 1-propenyl-	x	x	-	-

16	10.6	Indene	x	-	-	-
17	10.7	Phenol, 4-methyl-	x	-	-	-
18	10.8	Acetophenone	x	-	x	x
19	11.1	Benzene, 1-(1,1-dimethylethyl)-3-ethyl-	x	-	-	-
20	11.8	1-Dodecene	x	-	-	-
21	11.9	Azulene	x	-	-	-
22	13.4	Diphenyl	x	x	x	x
23	14.5	Diphenyldimethylsilane	x	x	x	x
24	14.7	2,2,4,4,6,8,8,10-nonamethyl-10-phenyl-1,3,5,7,9,2,4,6,8,10-pentaoxapentasilecane	x	x	-	-
25	15.0	Benzene, 1-methyl-2-[(3-methylphenyl)methyl]-	x	x	-	-
II	15.3	Unknown II (m/z 135, **239**, 253, 317, 332)	-	x	-	-
III	15.5	Unknown III (m/z 135, **239**, 253, 317, 332)	-	x	-	-
IV	15.6	Unknown IV (m/z 135, **239**, 253, 317, 332)	-	x	-	-
V	15.8	Unknown V (m/z 135, **239**, 253, 317, 332)	-	x	-	-
26	15.3	1,3-Bis(trimethylsiloxy)benzene	x	-	-	-
27	15.7	2,2,4,6-tetramethyl-4,6-diphenyl-1,3,5,2,4,6-trioxatrisilinane (cis)	x	x	-	-
28	16.8	**Unknown 28** (135, 193, **265**, 315, **329**, 358)	x	x	-	-
29	16.9	**Unknown 29** (135, 193, **265**, 315, **329**, 358)	x	x	-	-
30	18.0	2,4,6-Trimethyl-2,4,6-triphenyl-1,3,5,2,4,6-trioxatrisilinane(cis)	x	x	x	x
31	18.5	2,4,6-Trimethyl-2,4,6-triphenyl-1,3,5,2,4,6-trioxatrisilinane(trans)	x	x	x	x
VI	18.6-18.7	Unknown VI (m/z 180, 253, 319, **375**, 389, 453)	-	x	-	-
32	18.7	2,2,4,6,8-pentamethyl-4,6,8-triphenyl-1,3,5,7,2,4,6,8-tetraoxatetratrisilocane	x	x	-	-
33	19.4	2,2,4,4,6,8,8,10-octamethyl-6,10-diphenyl-1,3,5,7,9,2,4,6,8,10-pentaoxapentasilecane (cis)	x	x	-	-
34	19.5	2,2,4,4,6,8,8,10-octamethyl-6,10-diphenyl-1,3,5,7,9,2,4,6,8,10-pentaoxapentasilecane (trans)	x	x	-	-
35	20.3-20.7-20.9-21.0	2,4,6,8-tetramethyl-2,4,6,8-tetraphenyl-1,3,5,7,2,4,6,8-tetraoxatetrasilocane	x	x	x	-
36	25.2-25.5-26.0	2,4,6,8,10-pentamethyl-2,4,6,8,10-pentaphenyl-1,3,5,7,9,2,4,6,8,10- pentaoxapentasilecane	x	x	x	x

Spectroscopic characterization of the LSC

UV-Vis absorption spectroscopy was performed using a Cary 5000 UV-Vis-NIR spectrophotometer (Agilent) equipped with liquid or solid sample holder. Fluorescence spectra were measured at room temperature on a Horiba Jobin-Yvon Fluorolog®-3 spectrofluorometer

and equipped with a 450W xenon arc lamp, double-grating excitation, and single-grating emission monochromators. The fluorescence of LSC were recorded by using the Solid-Sample Holder and collecting the front-face emission at 30°. The quantum yield measurements in the solid state were obtained using a 152 mm diameter Quanta-phi integrating sphere, coated in Spectralon® and positioned on the optical path of the Horiba Jobin Yvon FluoroLogR-3 spectrofluorometer, placing the detector in right-angle mode (RA). The tests were carried out by inserting a circular portion of film with a diameter of 1 cm into the sample holder of the integrating sphere.

Fluorescence Lifetime Imaging (FLIM)

Fluorescence lifetime imaging (FLIM) were carried out on LSC using a Leica TCS SP5 inverted confocal microscope (Leica Microsystems, Wetzlar, GE) equipped with an external pulsed diode laser for excitation at 405 nm and 470 nm and a TCSPC acquisition card (PicoHarp 300, PicoQuant, Berlin, GE) connected to internal spectral detectors. Laser repetition rate was set to 40 MHz. Image size was 256×256 pixels and scan speed was usually set to 400 Hz (lines per second). The pinhole aperture was adjusted depending on sample fluorescence intensity. Samples were imaged using a 40×/NA 0.60 numerical aperture dry objective or with a 100x/1.3 NA oil immersion objective (Leica Microsystems). Emission was monitored between 580 and 660 nm using the built-in acousto-optical beam splitter detection system of the confocal microscope. The 256x256 images were acquired with a scan speed of 400 Hz (lines per second). Every measure was averaged between 3 frames. Acquisitions lasted until about 100–200 photons per pixel were collected, at a photon counting rate of 200–300 kHz. The decay curves were obtained from the lifetime images and fitted using PicoQuant SymPhoTime software for FLIM analysis.
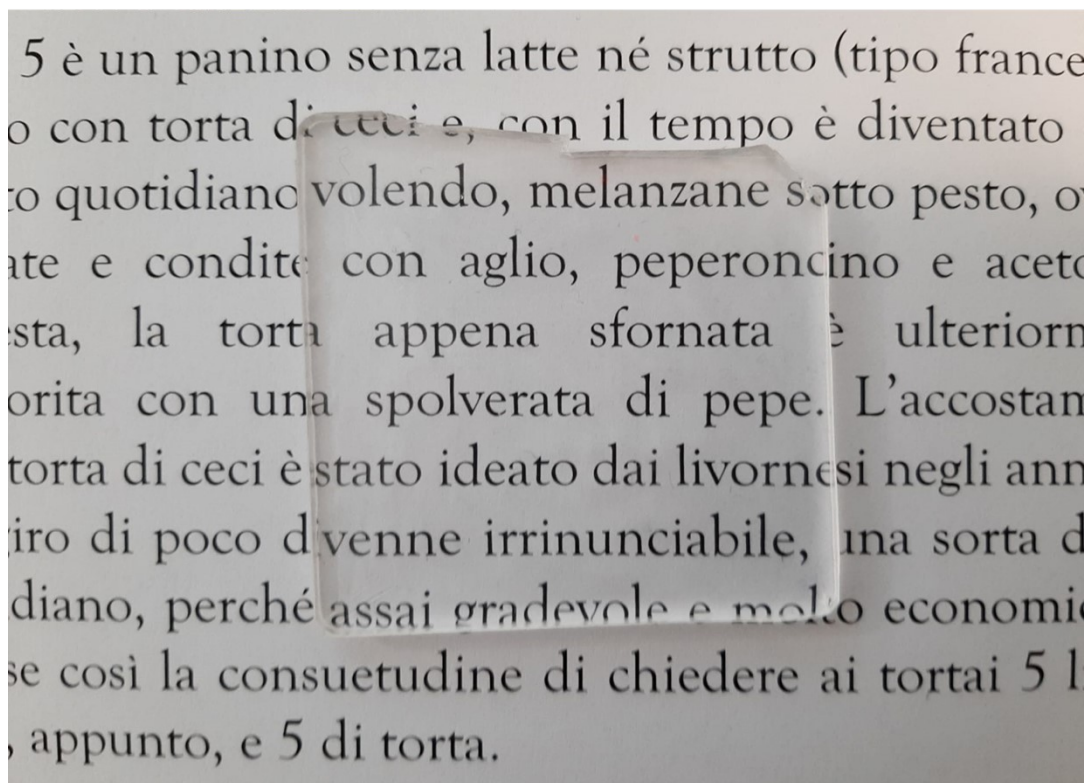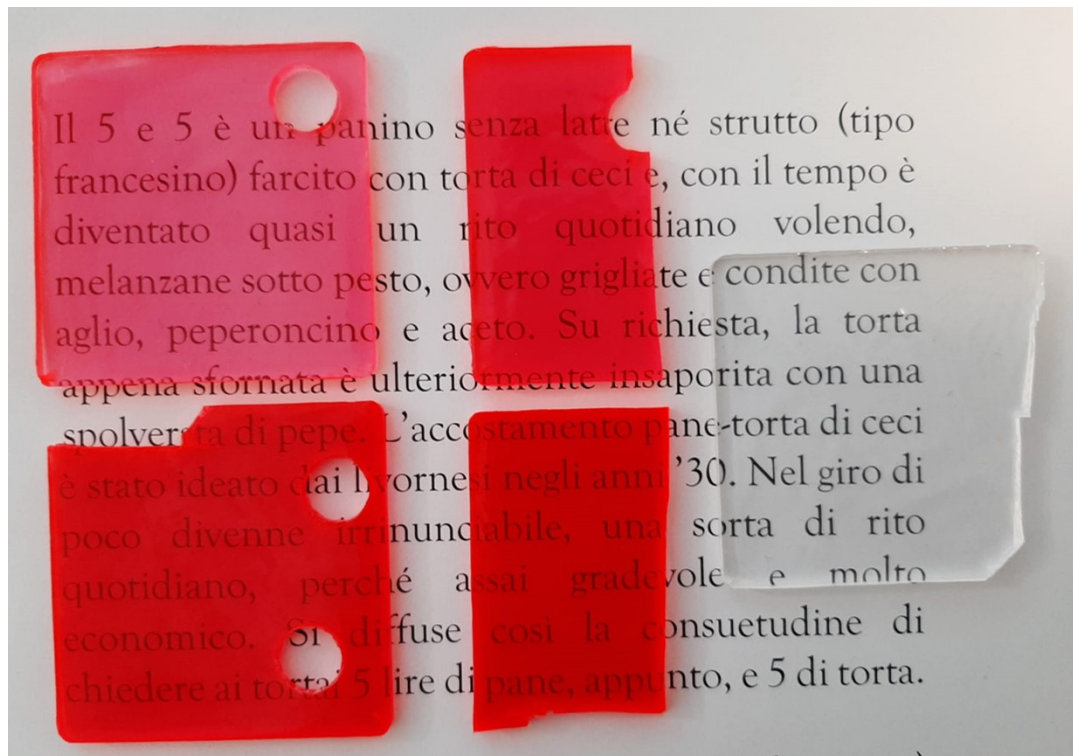
Table S2. Fluorescence Lifetime Imaging (FLIM) parameters

Sample	Fluorescence lifetime [ns]
LSC1_0	-
LSC1_50	5.52±0.02
LSC1_100	5.54±0.03
LSC1_150	5.60±0.03
LSC1_200	5.65±0.04
LSC2_0	-
LSC2_50	5.38±0.01
LSC2_100	5.39±0.01
LSC2_150	5.41±0.01
LSC2_200	5.44±0.05
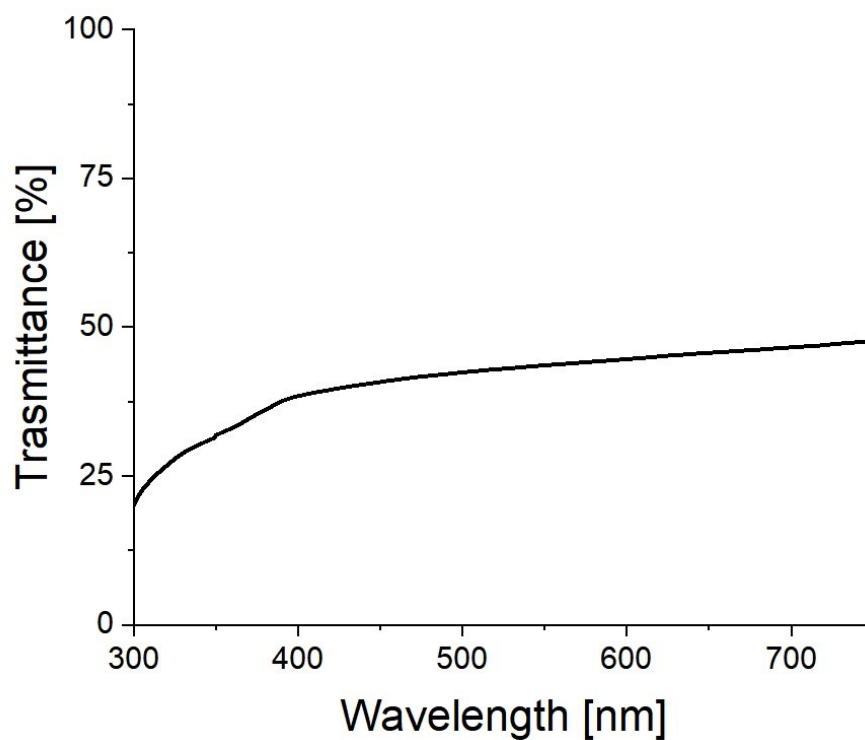
Figure S5. Transmittance of a 3mm-thick slab (unpolished) of polysiloxane

Figure S6. Photographs of LSC devices. In the top picture, from the top left to the bottom right, LSC2 series comprising 50 ppm, 100 ppm, 150 ppm and 200 ppm of dye; on the right, the slab containing no dye. The bottom picture is a close-up of the undyed slab. The noticeable holes and imperfections in the shape of the LSCs are due to the pieces employed for the different analyses performed during this study.

Figure S7. Photographs of a bent LSC device (LSC2_150)

Evaluation of internal (η_{int}), external (η_{ext}) photon efficiencies and device efficiency (η_{dev})

All the measurements were performed by using a commercially available system (Arkeo – Cicci research s.r.l.) containing a CMOS-based spectrometer with a symmetrical Czerny-Turner optical bench connected to an integrating sphere (Figure S8).
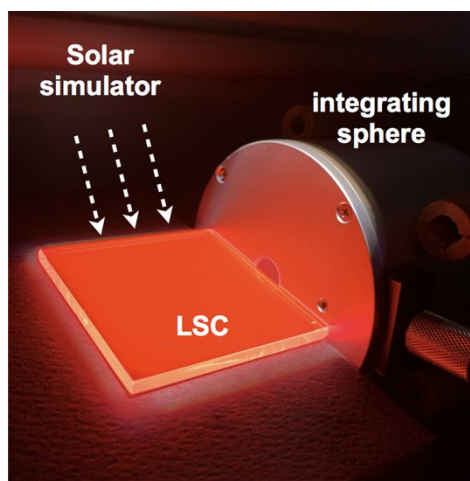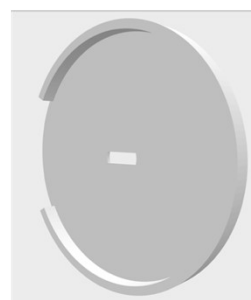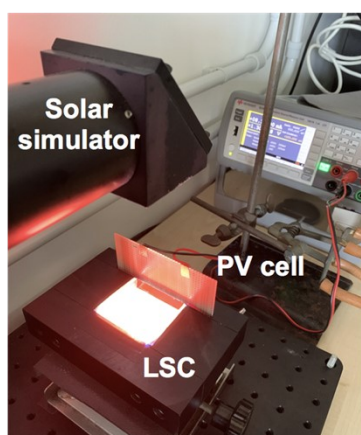
Figure S8. Photos of the experimental setup utilized for the determination of the photonic and device efficiencies

As illumination source an ORIEL® LCS-100 solar simulator 94011A S/N: 322 was utilized under controlled illumination (1 sun, AM 1.5G). An integrating sphere of 5 cm of diameter and 1 cm of aperture is placed along the edge of the glass plate. To avoid the collection of the stray light, the sphere was covered by an opaque plastic holder with a rectangular aperture of 1 cm (the diameter of the sphere) x 3 mm (i.e., the thickness of the LSC slab). The integrating sphere was moved along the side of the LSC until all the slab edge had been scanned. The spectrally-resolved edge output photon count was collected from the CMOS-based spectrometer and calibrated into optical power (W) and then in irradiance. Aimed at limiting reflections of unabsorbed light, an absorbing matte black background was placed in contact with the LSC

rear side. The fiber was kept close and perpendicular to the center of the LSC front surface to minimize the diverge of the excitation beam and to avoid the direct illumination of the integrating sphere. A series of 3-5 measurements were repeated in order align the integration sphere to collect the maximum single-edge output power.

The optical performances of LSC were evaluated in terms of the internal and the external photon efficiency (η_{int} and η_{ext}, respectively). η_{int} and η_{ext} were calculated from the equations S1 and S2:

$$\eta_{int} = \frac{\text{no. of edge} - \text{emitted photons}}{\text{no. of total absorbed photons}} = \frac{\sum_{i=1}^{i=n} \int_{\lambda_1}^{\lambda_2} P_{out,i}(\lambda)\frac{\lambda}{hc}d\lambda}{\int_{\lambda_1}^{\lambda_2} P_{abs}(\lambda)\frac{\lambda}{hc}d\lambda} = \frac{\sum_{i=1}^{i=n} \int_{\lambda_1}^{\lambda_2} P_{out,i}(\lambda)\frac{\lambda}{hc}d\lambda}{\int_{\lambda_1}^{\lambda_2} P_{in}(\lambda)(1-10^{-A(\lambda)})\frac{\lambda}{hc}d\lambda} \qquad \text{(Eq. S1)}$$

$$\eta_{ext} = \frac{\text{no. of edge} - \text{emitted photons}}{\text{no. of total incident photons}} = \frac{\sum_{i=1}^{i=n} \int_{\lambda_1}^{\lambda_2} P_{out,i}(\lambda)\frac{\lambda}{hc}d\lambda}{\int_{\lambda_1}^{\lambda_2} P_{in}(\lambda)\frac{\lambda}{hc}d\lambda} \qquad \text{(Eq. S2)}$$

Where:

a) $n = 4$, $\lambda_1 = 300$ nm and $\lambda_2 = 1100$ nm;

b) the number of edge emitted photons was obtained from the sum of the output power spectra measured for each edge of the LSC;

c) the number of total absorbed photons was obtained by convolution of the absorption spectrum of the LSC and the input power spectrum of the light source incident on the illuminated surface area of the LSC. Such value was also obtained by the difference between the incident input power and the transmitted power by the LSC.

d) The total number of photons incident on the front surface of the LSC was obtained from the input power spectrum of the light source incident on the illuminated surface area of the LSC.

For a blank LCE device (i.e. just the siloxane matrix), η_{int} and η_{ext} were calculated to be 36.5% and 1.5%, respectively.
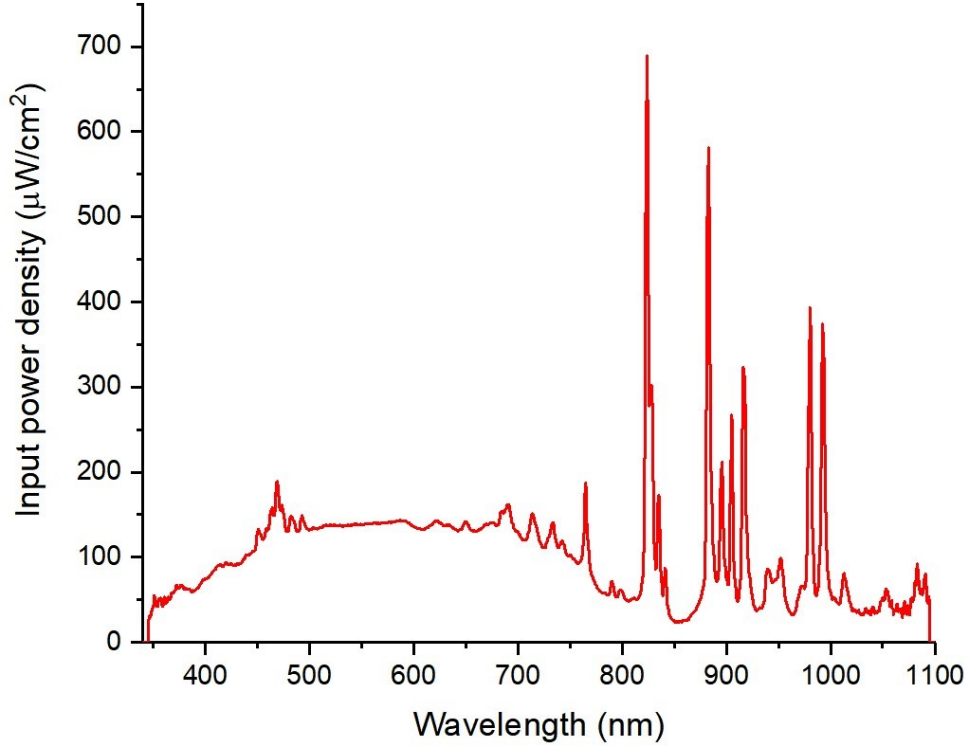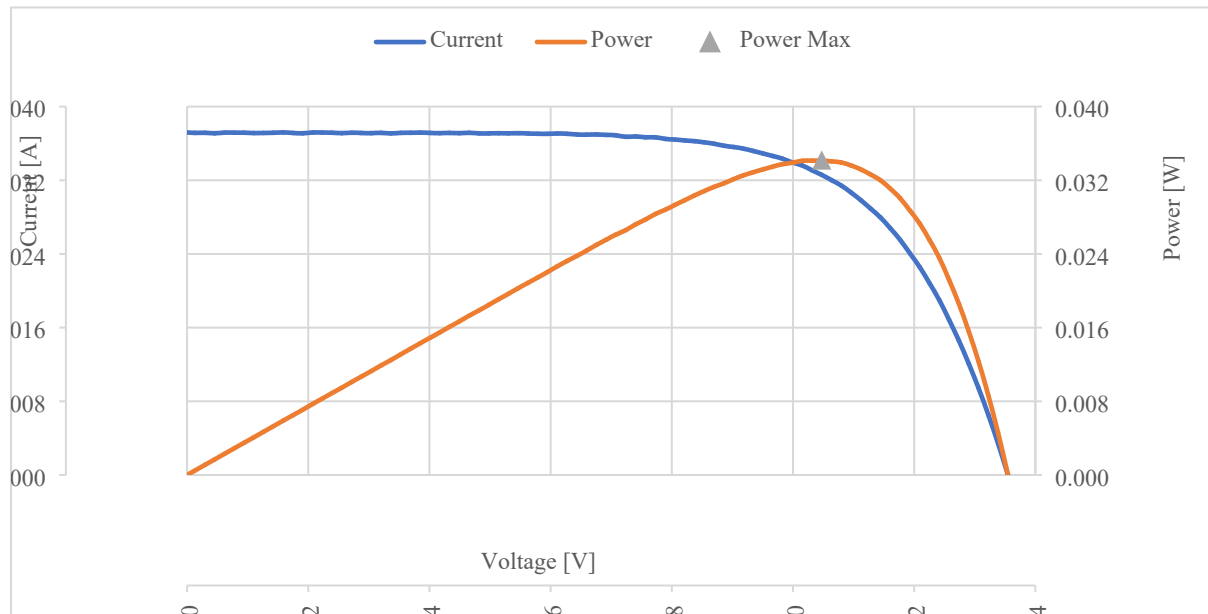
Figure S9. Input power density of the light source incident on the illuminated surface area of the LSC, $P_{in}(\lambda)$

The LSC efficiency is eventually determined connecting two Si-PV cells in series to an edge of the thin-film LSCs by using silicone grease. The performance of the assembled LSC-PV systems is assessed under standard illumination conditions by measuring the power conversion efficiency of the resulting LSC device (η_{dev}), defined as the electrical power effectively extracted from the PV cells (P^{out}_{el}) relative to the luminous power hitting the top surface of the LSC (P^{in}_{opt}):
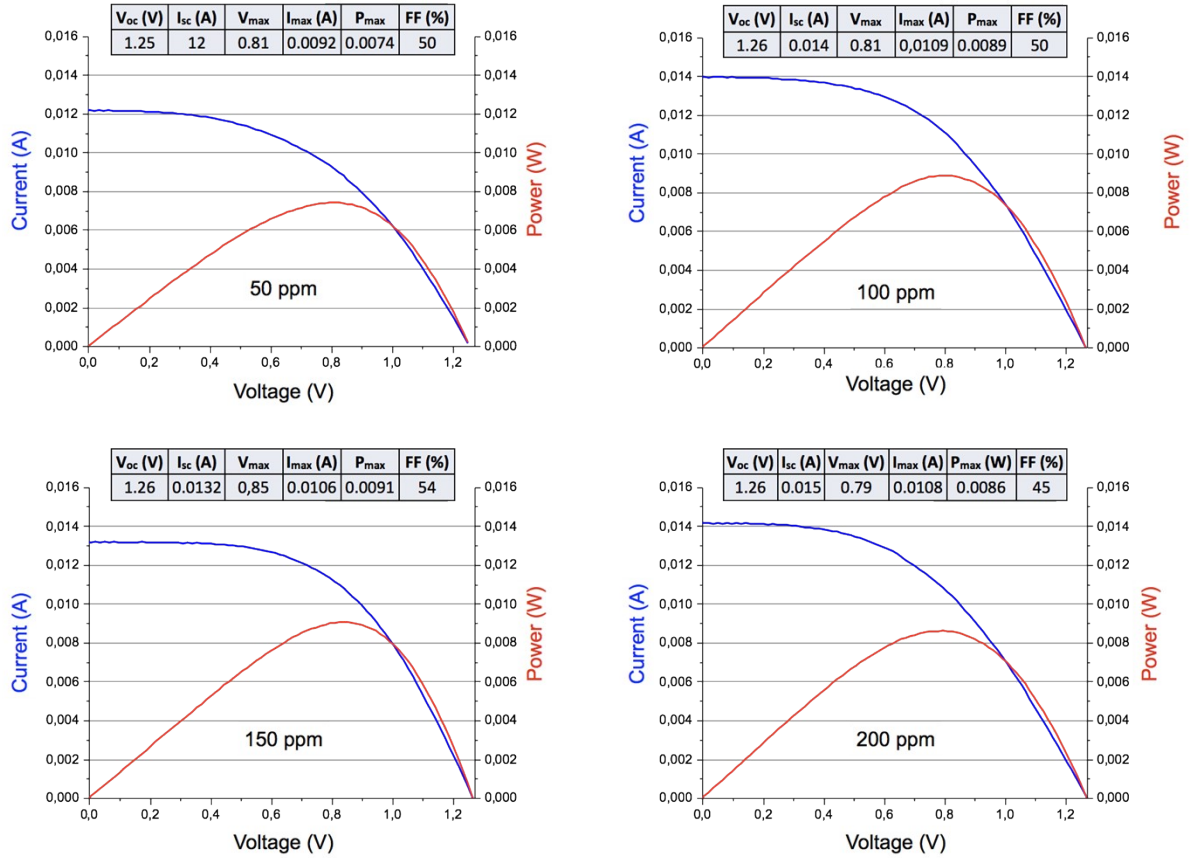
$$\eta_{dev} = \frac{P^{out}_{el}}{P^{in}_{opt}} = \frac{FF \cdot I_{SC} \cdot V_{OC}}{P^{in}_{opt} \cdot A_{LSC}} \quad \text{(Eq. S3)}$$

where FF, I_{SC}, and V_{OC} are the fill factor, short-circuit current, and open-circuit voltage of the edge-mounted PV cells, respectively, A_{LSC} is the front-illuminated area of the LSC device, and P^{in}_{opt} is the incident solar power density expressed in mW cm^{-2}.
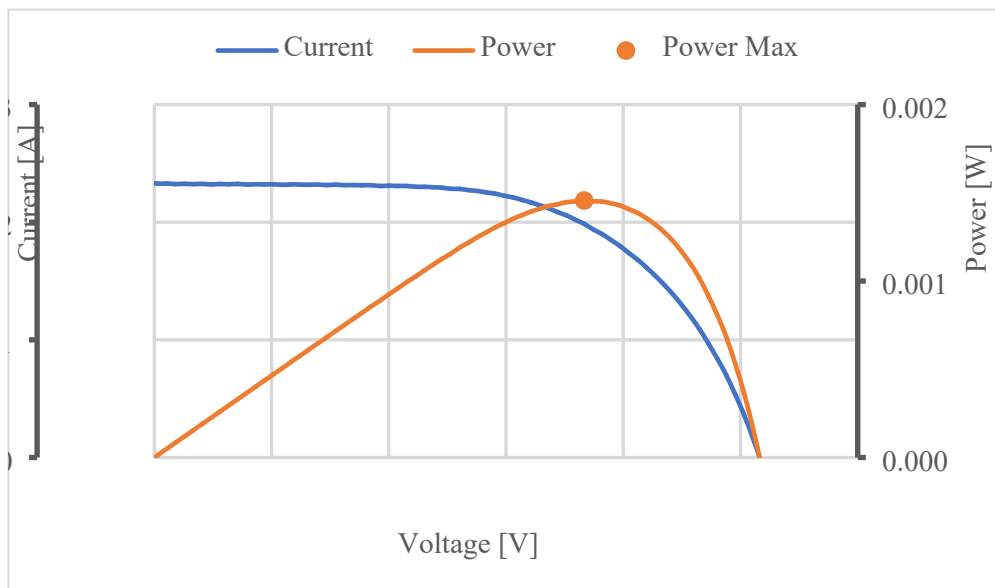
For the determination of η_{dev}, two PV cells IXYS KXOB25-12X1F (22 x 7 mm, $V_{oc} = 0.69$ V, $I_{sc} = 46.7$ mA, FF > 70%, $\eta = 25\%$) were connected in series and the current/voltage characteristics determined with a precision source/measure unit (Keysight Technologies B2900 Series). Silicon was used to grease the LSC edge. A black matte layer was placed beneath the LSC with an air gap of about 2.5 mm during the measurements.

Figure S10. Curve I-V of the monocrystalline silicon solar cell (IXOLAR cell)

V_{oc} (V)	I_{sc} (A)	V_{max}	I_{max} (A)	P_{max}	FF (%)
1.25	12	0.81	0.0092	0.0074	50

50 ppm

V_{oc} (V)	I_{sc} (A)	V_{max}	I_{max} (A)	P_{max}	FF (%)
1.26	0.014	0.81	0,0109	0.0089	50

100 ppm

V_{oc} (V)	I_{sc} (A)	V_{max}	I_{max} (A)	P_{max}	FF (%)
1.26	0.0132	0,85	0.0106	0.0091	54

150 ppm

V_{oc} (V)	I_{sc} (A)	V_{max} (V)	I_{max} (A)	P_{max} (W)	FF (%)
1.26	0.015	0.79	0.0108	0.0086	45

200 ppm

Figure S11. Curve I-V of the prepared LSC at different FC546 concentration (ppm)

Figure S12. Curve I-V of undoped LSC. $\eta_{dev}= 0.09 \pm 0.01$ (calculated on three measures)
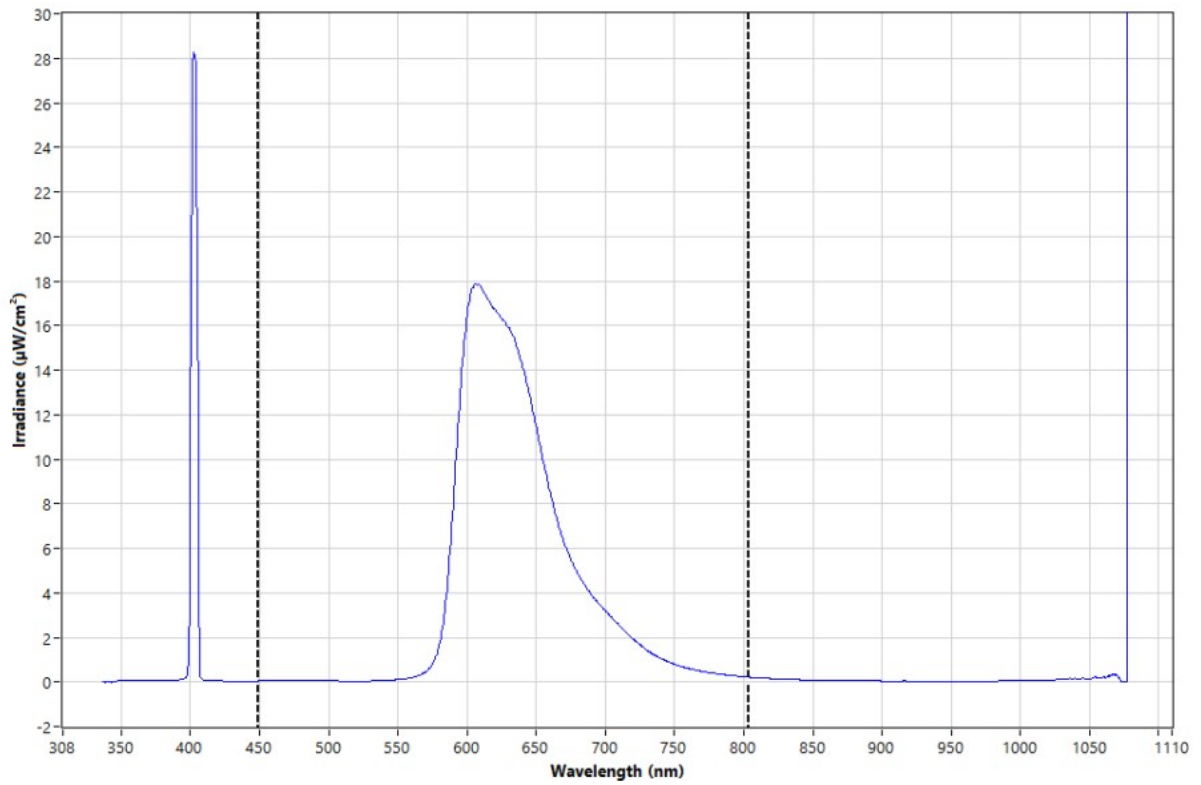
Figure S13. Edge emission from LSC2 150 ppm measured by irradiating the centre of the slab with a green laser (400 nm) over a circle with a diameter of 1 cm.